

JAAS

Accepted Manuscript



This is an *Accepted Manuscript*, which has been through the Royal Society of Chemistry peer review process and has been accepted for publication.

Accepted Manuscripts are published online shortly after acceptance, before technical editing, formatting and proof reading. Using this free service, authors can make their results available to the community, in citable form, before we publish the edited article. We will replace this *Accepted Manuscript* with the edited and formatted *Advance Article* as soon as it is available.

You can find more information about *Accepted Manuscripts* in the [Information for Authors](#).

Please note that technical editing may introduce minor changes to the text and/or graphics, which may alter content. The journal's standard [Terms & Conditions](#) and the [Ethical guidelines](#) still apply. In no event shall the Royal Society of Chemistry be held responsible for any errors or omissions in this *Accepted Manuscript* or any consequences arising from the use of any information it contains.

Evaluation of the Analytical Performances of Valve-based Droplet Direct Injection System by Inductively Coupled Plasma-Atomic Emission Spectrometry

Kaori Shigeta,^{*a} Yuki Kaburaki,^b Takahiro Iwai,^b Hidekazu Miyahara^b and Akitoshi Okino^b

Cite this: DOI:
10.1039/x0xx00000x

Received 00th January 2012,
Accepted 00th January 2012

DOI: 10.1039/x0xx00000x

www.rsc.org/

We have developed a sample introduction system using a magnetic valve type dispenser, named "droplet direct injection nebulizer (D-DIN)". In the case of D-DIN, sample solution is directly injected as a single droplet or series of droplets into the plasma. Droplet volume can be controlled across a wide range of droplet size from 700 pL (110 μm) to 100 nL (580 μm) by changing the inner diameter of the nozzle tip, back pressure and valve open time. The D-DIN system additionally enables direct injection of cells contained in a droplet into the plasma. In this study, the droplet system was optimised, and droplet characterization and analytical performances by emission profiles were investigated. When the emission intensities of 15 nL-volume droplets were measured by side-on observation, the detection limits of Na, Mg and Sr were 20.3 pg (1.35 μg ml⁻¹), 56.5 pg (3.77 μg ml⁻¹) and 20.6 pg (1.37 μg ml⁻¹), respectively. Finally, a single droplet containing yeast cells was directly introduced into ICP and the emission profile of Na was measured with a satisfactory signal to noise ratio.

Introduction

Many trace metals in biological fluids and organs are incorporated into proteins, known as metalloproteins. Some of them operate as a biological catalyst in the regulation of reactions and physiological functions in biological cells and organs.¹ Distribution of major-to-ultratraces elements in biological fluids, cell and organs was established as one of the main research subjects for metallomic studies.² Distribution of these elements may provide information about health and disease of primary importance in medical diagnosis, and may help in the design of chemotherapy drugs.³ Haraguchi *et al.* performed the first study to measure metals in single or three salmon egg cells.^{2,4} The quantitative data for 74 elements were reported in a concentration range from 0.359 % for P to 0.00037 ng g⁻¹ for Tm on the basis of three salmon egg cells.⁴ However, it is still difficult to measure trace elements in a single cell because of the limited amount of sample. There is a strong requirement for new and more advanced analytical techniques.

Scott Tanner's group from the University of Toronto has shown for the first time a single cell analysis by using a homemade mass spectrometric cytometer (MSC)⁵ based on an inductively coupled plasma mass spectrometers (ICP-MS). In the work of Scott Tanner's group, the cells were detected indirectly in an immunoassay by use of a metal labeled

antibody.⁶ For sample introduction a conventional micro-concentric nebulizer in a desolvation system was applied. The ICP-MS used for the MSC is based on a very specific time of flight instrument, which only allows measurement of all elements above 100 Da. Thus it has not yet been applied to measure the natural composition of essential elements and metals in single cells. The direct label-free analysis of single cells by ICP-MS has been first reported by Sam Houk's group.⁷ They measured the signal of U incorporated intrinsically into *Bacillus subtilis* using a micro-concentric nebulizer and operated the ICP- sector field mass spectrometer (SFMS) with an integration time of 4 ms to investigate the behavior of single cells and observed U⁺ spikes for intact bacteria. Recently, a single particle methodology using a glass concentric nebulizer was applied to algae⁸, yeast⁹ and nanoparticles.¹⁰

On the other hand, monodisperse droplet generators have been used to observe the production of atoms and ions for flames and plasmas. Hieftje *et al.* developed a system to generate droplets on demand by mechanically disturbing a liquid stream transported through a capillary.¹¹ The developed system was applied for the observation of atoms and ions for flame. For injection of individual droplets, and monodispersed and isolated droplets into an ICP, French *et al.* designed a monodisperse dried microparticulate injector (MDMI).¹² This system consists of a piezoelectrically driven micro pump,

1 which the flow rate can be varied by utilizing an appropriate
2 variable-frequency square wave pulse generator from a single
3 droplet (e.g., 57 μm diameter droplet size, 0.1 nL diameter
4 droplet volume) up to 6000 Hz ($0.58 \mu\text{L s}^{-1}$).¹² Olesik *et al.*
5 reported for the first time spatially and temporally resolved
6 measurements of emission intensities using a MDMI.¹³
7 Emission profiles were measured from a single drop, and its
8 heights and peak areas had a relative standard deviation of 1–
9 6%. Groh *et al.* applied a commercial piezoelectric droplet
10 generator to ICP-AES to investigate desolvation and
11 atomization in an ICP.¹⁴

12 In the last couple of years, a micro-droplet generator
13 (μDG) are becoming popular for sample introduction system in
14 ICP-MS. Niessen *et al.* have developed a home-built aerosol
15 generator given the name “droplet on demand” based on a
16 modified thermal inkjet cartridge.¹⁵ In our previous paper^{16, 17}
17 we have optimized a micro droplet generator (μDG) for sample
18 introduction into an ICP-SFMS, which was also applied in the
19 work of Gschwind *et al.*¹⁸ and Franze *et al.*¹⁹ for analysis of
20 single metallic nanoparticles. We have shown for the first time
21 that semi-metals and metals were investigated in single cells by
22 using ICP-SFMS with high time resolution.¹⁷ However, some
23 problems related with this application still remain unanswered.
24 First problem is that cells might be destroyed during the high
25 pressure shock waves produced for droplet generation.
26 Exploding cells in the tip capillary would cause memory effects.
27 Second problem is that clogging and the trajectory errors occur
28 when the droplets containing a cell with several tens μm in
29 diameter are injected. It would be a rather limitation because a
30 typical size of biological cells commonly used in experimental
31 biology is ranging from a few μm to several tens μm in
32 diameter. Fortunately, these have not yet been observed and can
33 be related to the fact that the yeast cells used here are enough
34 small (about 4 μm) and robust.¹⁷ For stable droplet injection
35 containing a cell, the droplet diameter must be optimised to fit
36 the cell diameter but a piezo type dispenser generate only
37 similar size of droplet as nozzle tip diameter. In addition, it is
38 hard to change a nozzle tip because a glass capillary with a
39 nozzle tip is surrounded by a piezo actuator. The fact also
40 makes maintenance difficult when a capillary is clogged.

41 For all the considerations, we developed new sample
42 introduction system using a magnetic valve type dispenser
43 named droplet direct injection nebulizer (D-DIN) system.^{20,21} In
44 our previous work, the D-DIN system were applied to ICP
45 measurement system, the emission intensities of analyte were
46 measured from droplets containing a sample solution. However,
47 it was difficult to introduce the droplets into the centre of the
48 plasma, and emission intensities were unstable in some cases.
49 The present work has three main goals: (i) to improve the
50 stability of droplet injection into the plasma; (ii) to show
51 droplet characteristics and analytical performances such as
52 signal intensity, precision and LODs from emission profiles;
53 and (iii) to present a principle experiment of direct injection of
54 a high amount of cell.
55
56
57
58
59
60

Experimental

Reagents and samples

The analytical performance of D-DIN-ICP- atomic emission spectrometer (AES) was evaluated using a multi-element solution prepared from standard solution ($100 \mu\text{g ml}^{-1}$ Na, Mg, Sr, Kanto Chemical Co., Inc., Japan). Standard solution was diluted using ultra-pure water ($>18.4 \text{ M}\Omega \text{ cm}^{-1}$) (Japan Millipore K.K., Tokyo, Japan). Sensitivity tuning of D-DIN-ICP-AES was also conducted using the same multi-element solution. Dry yeast (Oriental yeast co., Ltd., Tokyo, Japan) was used for direct injection of cells. To determine the concentration of yeast cells, dry yeast was digested with nitric acid (70%) and hydrogen peroxide (30%) (both were of electronic laboratory grade, Kanto Chemical Co., Inc., Japan). Samples of standard calibration were prepared by diluting a standard solution of Na ($1000 \mu\text{g ml}^{-1}$; AAS grade, Kanto Chemical Co., Inc., Japan) with ultra-pure water.

Element analysis of digested yeast sample

To determine total Na in yeast cells, 1.00 g of yeast sample was digested using a microwave oven (Multiwave 3000, PerkinElmer Japan Co., Ltd., Yokohama, Japan) after the addition of 20 ml nitric acid and 0.8 ml hydrogen peroxide. When samples were had been completely digested, indium was added to a final concentration of 50 ng ml^{-1} for use as an internal standard, and the weight was adjusted to 100 mL (a dilution factor of 100) by ultra- pure water. Na was determined by an ICP-MS instrument (ELAN DRC-e, Perkin Elmer Japan Co., Ltd., Yokohama, Japan), equipped with a conventional nebulizer (Conical Nebulizer 1 mL min^{-1} , Glass Expansion, West Melbourne, VIC, Australia).

Direct injection of standard solution and yeast cells by D-DIN-ICP-AES

For direct injection of standard solution, $10 \mu\text{g mL}^{-1}$ Na, Mg and Sr standard solution was prepared by diluting a multi-element solution using ultra-pure water. For direct injection of yeast cells, 500 mg of dry yeast was diluted with ultra-pure water up to 50 mL (a dilution factor of 100). In order to minimize any alternation of yeast cells, yeast samples were diluted before analysis. The number of yeast cells in a single droplet was calculated from the concentration of yeast cells in the diluted yeast sample solution. Concentration of yeast cells was counted by using a cell counting plate and a microscope.

Instrumentation

Droplet direct injection nebulizer (D-DIN) system

The same setup of D-DIN system in our previous paper²¹ was used to generate droplets. Fig. 1 shows the schematics of the D-DIN system. A dispenser device (MJ-020 Standard Type, Mect Corporation, Osaka, Japan), which consists of dispenser head equipped with magnetic valve, control unit, and sample solution container, was used as a droplet dispenser. The following

parameters affected the droplet volume: applied backpressure (< 0.15 MPa), and valve open time (0.04 - 10 ms), controlled by the control unit. While a back pressure (0.001 - 0.200 MPa) was applied to the sample container, the sample solution was transported to the dispenser head, and injected by opening the magnetic valve with a short pulse. The pulse was provided by a function generator (AFG3102, Tektronix Inc., Tokyo, Japan), and transmitted to the control unit through a metal-oxide-semiconductor field-effect transistor (Mofset) (ZVNL 120A, Diodes Inc., Taipei, Taiwan) used for amplifying and switching electronic signals. The number of droplets introduced could be controlled within a range from a single droplet to 5000 droplets sec^{-1} . However, droplet introduction frequencies were set from 0.1 to 10 Hz during experimental investigation to avoid blinking and extinction of plasma. In this study, stainless steel tips (30, 50, 100 μm i.d., 30 mm long, Mect Corporation, Osaka, Japan) and a fused-silica tip (30 μm i.d., 500 mm long, New Objective, Inc., Woburn, USA) were used as a nebulizer nozzle tip to reduce droplet volume and to obtain fine droplets without droplet satellites. The silica tip was cut to 15 mm by a diamond-blade cleaving tool.

The velocity as the mean value of moving distance was measured by taking photographs with a high-speed video camera (500 frames sec^{-1} , MotionScope, Redlake MASD Inc., San Diego, CA, USA) every 2 msec.

Design of ICP-torch for the D-DIN

An ICP-torch designed for the D-DIN system²¹ was modified for more stable transportation of droplet. Design of ICP-torch was described in Fig.2. The torch had a three-layer tube structure and was made from quartz glass. The nebulizer nozzle tip was directly mounted into the ICP torch by a laboratory design connector. In this study, a connector and spacer made from polytetrafluoroethylene (PTFE) were designed additionally to distribute the carrier gas through the centre of spacer if necessary. The carrier gas flow in inner tube is focused by the spacer, and it enables droplet to be introduced into the centre of the plasma. The plasma gas is introduced into the middle layer from a tangential direction through the gas inlet, and the auxiliary gas is not needed for this torch. In the outer layer, the cooling gas is introduced, and is exhausted in the axial direction cylindrically around the plasma.

In addition, the torch has two significant differences from a conventional Ar-ICP torch: (1) a smaller plasma gas inlet which creates a higher initial gas velocity; and (2) a shorter distance between the plasma gas inlet and the plasma generation region which prevents a reduction in vortex flow velocity.²²⁻²⁶ The torch has the advantage that a stable Ar ICP can be generated from 200 to 1400 W RF power with a plasma gas flow rate of 3 to 15 L min^{-1} and a cooling gas flow rate of 20 L min^{-1} .^{25, 26} In this study, the ICP was operated with a RF power of typically 1000 W and a plasma gas flow rate of 13 to 15 L min^{-1} , and cooling gas was used to avoid the torch melting when the radio frequency wave (RF) power was higher than 1000 W. The other experimental facilities of ICP source, such

as an RF generator, impedance matching network and gas introduction, have been described in previous papers.^{22, 26}

Spectrometer and data acquisition

The optical detection system consists of a spectrometer (500-mm focal length, 0.0270-nm resolution, Czerny-Turner) with a photoelectron multiplier (PMT) (R928, Hamamatsu Photonics Co., Ltd., Shizuoka, Japan). The spectral emission from the excited atoms was imaged by a quartz lens ($f=101.7$ mm, aperture: 40 mm) onto a fibre, and was introduced to the entrance slit of a monochromator with a photomultiplier. The experimental arrangement is shown in Fig. I (ESI). In the case of side-on observation, the emission intensity was measured at a position of 0 mm above the load coil (A.L.C.). The lens was set at a position of 200 mm (2f) from the centre of the plasma, and a one-to-one image was focused at a position of 200 mm (2f). In the case of end-on observation, the lens was set at a position of 300 mm (3f) from a position of 0mm A.L.C., and a half image was focused at a position of 150 mm (3/2f). The alignment was performed by adjustment of the imaging of ICP and the optical fibre to the maximum peak height of analyte in multi-element solution. The photomultiplier signal was digitized and stored by a digital storage oscilloscope (TDS-680B, Sony/Tektronix Corp., Tokyo, Japan). A time resolution of 40 μs was used to detect transient emission signals from a single droplet. The sample rate was 25 kHz.

Results and discussion

Characteristics of droplets

A piezo-based droplet dispenser has been applied for analysis of selenized yeast cells.¹⁷ However, as already described earlier, there still remain two main problems to be resolved: (i) cell damage from piezoelectric shock wave; (ii) clogging and the trajectory errors occur by injection of a cell with several tens μm in diameter. In the D-DIN system, a valve-based droplet dispenser is used, and does less damage to cells. Moreover, the nebulizer nozzle tip is easily-exchangeable, and the variety of sizes in the nozzle tips can be chose to fit on cellular size. The parameters of sample introduction conditions — the nebulizer nozzle tip inner diameter, back pressure, and magnetic valve opening time and droplet introduction frequency — can be changed. The droplet volume as a function of the parameters was described in our previous paper.²¹ The volume and the diameter of the droplet was calculated from the density of water (0.998 g mL^{-1} at 20 °C) and the mean mass of a single droplet. The mean mass of a single droplet was calculated from a mass of 1200 droplets. A threshold pressure of 0.05 MPa was required for stable droplet injection. Using this system, the droplet volume was changed from 700 pL (110 μm) to 100 nL (580 μm). In the case of 700 pL (110 μm), droplet volume, nozzle tip inner diameter, back pressure and valve time were set at 30 μm , 0.02 MPa and 0.5 msec.

The sample droplet should be introduced linearly into the plasma. However, the trajectory of droplet would be shifted

considerably if its ejection speed is too low. Thus, droplet velocity as a function of back pressure at various valve open times was evaluated (Fig. 3 (a)). When nozzle tip diameter was 100 μm i.d., droplet velocity increased from 0.55 to 14 m/s with a corresponding increase in back pressure. On the other hand, droplet velocity was not altered by changing the valve open time. Next, the droplet velocity as a function of back pressure at various nozzle tip diameters was measured (Fig. 3(b)). The valve open time was set at 0.5 ms. The droplet velocity increased from 2.5 to 16 m/s with a corresponding increase in back pressure. There were no marked changes in nozzle tip diameter. Based on these results, it was concluded that the velocity of droplets can be controlled by the back pressure alone. The sample droplet velocity obtained by a typical nebulizer system and DIHEN are 5.3 m s^{-1} and 30 - 40 m s^{-1} , respectively. Therefore, the D-DIN allowed samples to remain in the plasma for a longer time. The velocity could be increased by a carrier gas flow around the droplet.

Observation of emission profile from water droplets

In the D-DIN system, as I discussed earlier, the droplet volume was changed from 700 pL (110 μm) to 100 nL (580 μm) but the droplet sizes is larger than that generated from piezo-based droplet dispenser. Thus, emission profiles were observed by introducing droplets generated from ultra-pure water. For droplet condition, nozzle tip inner diameter, backpressure and valve open time were set at 100 μm , 0.05 MPa and 0.5 ms, respectively, and the volume of droplet was 5.5 nL (220 μm). Droplet introduction frequency was 10 Hz. For plasma condition, RF power and Ar gas flow was 1000 W and 14 L min^{-1} , respectively. For the spectroscopic experiment, the argon atomic line (Ar I 425.11 nm and Ar I 426.62 nm) and H_β line (486.13 nm) were measured by side-on observation. Fig. 4 shows the Ar atomic line (Ar I 425.11 nm), H_β line (486.13 nm) and Ar excitation temperature with droplet injection. The excitation temperature of Ar was calculated from emission intensities of Ar I 425.11 nm and 426.62 nm.²⁷ The droplets were injected at 0, 100, 200 and 300 msec. There was a fixed time lag between the timing of sample injection and detection of the H_β line. This delay was related to the time droplets required to reach the plasma and become ionized after sample injection. The H_β line was increased at the same frequency of droplet injection. With an increase of H_β line Ar excitation temperature was decreased momentarily. This suggested that the population density of the excited Ar atoms decreased due to desolvation of a droplet in the plasma. In addition, the excitation temperature overshoot the value achieved before droplet injection. This effect might be due to better heat conductivity caused by hydrogen.²⁸

Fig. 5 shows variation in the emission profile of the H_β line as a function of RF power, valve open time and back pressure. In Fig. 5 (a), for droplet condition, nozzle tip diameter, backpressure and valve open time were 100 μm , 0.05 MPa and 0.5 ms, respectively, and the droplet volume was 5.5 nL (220 μm). The emission intensities were measured by side-on observation. When RF power was 1000 W, the emission intensity almost

reached a plateau. In Fig. 5 (b) and (c), RF power was set at 1000 W. Emission intensities increased with increasing valve open time and back pressure. The droplet volume at valve open time of 0.5, 2, 5 and 10 msec was 5.5, 12, 27 and 51 nL, respectively, and the droplet volume at back pressure of 0.04, 0.05, 0.07 and 0.10 MPa was 5.0, 5.5, 6.5 and 7.1 nL, respectively. However, the emission intensity did not proportionally increase with droplet volume. This showed that the H_β line was not completely excited due to the large droplet volume.

Atomization of elements contained in droplets

To investigate the atomization of elements in droplets with carrier gas flow, droplets containing Na standard solution were introduced into plasma and measured by end-on observation. To avoid the spacer mounted on ICP-torch melting, RF power was set at 700W. For droplet condition, nozzle tip inner diameter, backpressure and valve open time were 50 μm , 0.038 MPa and 2 ms, respectively, and the droplet volume was 4.7 nL (210 μm). A sample solution of 10 $\mu\text{g mL}^{-1}$ Na standard solution was used. Fig. 6 shows the emission profile of the sodium atomic line (588.99 nm) and H_β line (486.13 nm) by end-on observation, as a function of carrier gas flow rate (0 - 0.8 L min^{-1}). At 0.4 L min^{-1} of carrier gas flow, a better peak shape was observed. The start of desolvation can be taken from the rising of the H_β emission. After the H_β intensity achieved its maximum, the sodium atomic line intensity rose. Atomization of sodium started after the end of desolvation, which can be seen from the decreasing of H_β emission intensity. The duration for desolvation was then about 9 ms, and is relatively long due to the large droplet volume compared to the sample residence time in the plasma. To achieve effective analysis of the droplet sample, we currently developed an injection gas heating system²⁹ based on the desolvation system as is described before.^{17,18} It is expected that the duration for desolvation would be shorter by applying the injection gas heating system to D-DIN.

Evaluation of analytical performances of the D-DIN-ICP-AES

Analytical performances of the D-DIN-ICP-AES, such as intensity and precision LODs, were investigated. For this experiment, a fused-silica tip was used as a nebulizer nozzle tip. In the case of a fused silica tube, it was possible to generate droplets reproducibly due to the elaborate edge of the tip. The fused silica tube was cut to 15 mm to generate smaller droplets. Nozzle tip diameter, backpressure and valve open time were 30 μm (silica tip), 0.10 MPa and 2.0 ms, and droplet volume was 15 nL (300 μm). RF power was 700 W. The carrier gas flow rate was 0.4 L min^{-1} , which optimized in previous section. Fig. II (ESI) gives the emission profiles of Na I 588.99 nm, Mg II 280.27 nm and Sr II 407.77 nm, with 10 $\mu\text{g mL}^{-1}$ Na, Mg and Sr standard solution. Emission intensities were measured by side-on observation. Emission signals increased with the introduction of sample solution by D-DIN. As it took some seconds to stabilize the background signal after injection of a droplet, the peak widths of Na, Mg, and Sr at 80% maximum of

1 peak height were compared, and found to be 13 msec, 11 msec
2 and 10 msec.

3 To evaluate the stability of droplet introduction, at the same
4 conditions, the emission signal was measured at a frequency of
5 0.5 Hz for 20 sec. These results are shown in Fig. 7. Droplets
6 were injected at low frequencies in order to stabilize the
7 background signals arising from a droplet. The standard
8 deviation of Na, Mg and Sr was calculated at peak height and
9 for peak area. The standard deviation calculated for peak area
10 was an improvement compared to those calculated for peak
11 height, which can be related to the scattering of droplets in
12 plasma. Table 1 summarizes the detection limits and the
13 absolute detection limits for Na, Mg and Sr. The S/N was
14 calculated from the peak area. Detection limit was defined as
15 the concentration when the S/N is 3. Absolute detection limit
16 (pg) was calculated by multiplying the detection limit ($\mu\text{g mL}^{-1}$)
17 by droplet volume (nL). The detection limits of Na, Mg and Sr
18 were 20.3 pg ($1.35 \mu\text{g mL}^{-1}$), 56.5 pg ($3.77 \mu\text{g mL}^{-1}$) and 20.6 pg
19 ($1.37 \mu\text{g mL}^{-1}$), respectively. For comparison, detection limit in
20 ICP-AES equipped with pneumatic nebulizer³⁰ were also listed
21 in Table 1. The absolute detection limit was calculated to be
22 500 pg, 30 pg and 30 pg for an uptake rate and introduction
23 time of 0.8 mL/min and 20 s, respectively. When the D-DIN
24 was used, the absolute detection limits were almost at same
25 level when compared to a conventional nebulizer.

26 Direct injection of yeast sample

27 For direct injection of yeast cells by single droplet, a droplet
28 containing yeast cells was directly introduced into the plasma
29 using D-DIN. 0.44 g of dry yeast sample (2.5×10^{10} cells g^{-1})
30 was diluted with ultra-pure water, and the volume was adjusted
31 to 50 mL (a dilution factor of 110). Yeast cell numbers in a
32 single droplet was estimated from both droplet volume and
33 yeast cell numbers in the diluted yeast sample solution. In the
34 case of 15 nL of droplet volume, yeast cell numbers in a single
35 droplet corresponded approximately to 3300 yeast cells. These
36 results are shown in Fig. 8. Emission intensity of Na was
37 measured in a single droplet containing yeast cells. To estimate
38 the quantity of elements in a single droplet, digestion of the dry
39 yeast sample was carried out after HNO_3 and H_2O_2 were added.
40 The digested samples were analysed by ICP-MS. The
41 concentration and amount of Na in cells was $961 \pm 77 \mu\text{g mL}^{-1}$
42 and 37.9 ± 3.0 fg, respectively. The total amount of elements in
43 a single yeast cell was calculated by dividing the concentration
44 of elements in a single yeast cell by the yeast cell number / dry
45 weight of yeast. From these results, the concentration of Na in a
46 droplet containing 3300 yeast cells was calculated as $8.4 \mu\text{g mL}^{-1}$
47 if it is assumed that all of the cells are the same. Thus, in
48 the case of a 15 nL-droplet volume, the absolute amount of Na
49 corresponded to 125 pg. With the single shot injection of
50 sample droplets containing yeast cells, a strong sodium
51 emission was observed with sufficient S/N. These results were
52 almost comparable to the signal intensity of these elements as
53 measured by direct injection of yeast cells.

Conclusions

To enable the highly sensitive analysis of cell suspension, we developed the D-DIN system. The volume of the droplets was controlled by the nozzle tip diameter and the applied back pressure. Using this system, the droplet volume was changed from 700 pL (110 μm) to 100 nL (580 μm). Droplet velocity can be controlled from 0.55 to 16 m/s with a corresponding increase in back pressure. For a single droplet with a 15-nL volume, the absolute detection limits of Na, Mg and Sr were 20.3 pg, 56.5 pg and 20.6 pg, respectively. Furthermore, a droplet containing yeast cells was directly introduced into the plasma. With a single shot droplet that included about 3300 yeast cells, a mass signal of Na was observed. However, its detection sensitivity was not found to be sufficient for the detection of trace elements (ppb level) in a single cell. To improve the detection sensitivity, the solvent load should be reduced by desolvation. Therefore, we currently developed an injection gas heating system. The operation condition according to droplet size would be optimized. Also we would apply the D-DIN system to ICP-MS.

Acknowledgements

The present research, entitled “World’s First Direct Single Cell Analysis using Inductively Coupled Plasma Mass Spectrometer”, was supported by Agilent Technologies Foundation Research Project Gift. We are grateful to Dr. Takashi Kondo (Agilent Technologies) for providing valuable information about instrumental and operational details of ICP ion source. The present research was also supported by a research fellow of the Japan Society for the promotion of young scientists at the Japan Society for the Promotion of Science (JSPS). We thankfully acknowledge many fruitful discussions with Dr. Norbert Jakubowski (BAM Federal Institute for Materials Research and Testing).

Notes and references

a Research Institute for Environmental Management Technology, National Institute of Advanced Industrial Science and Technology (AIST), 16-1 Onogawa, Tsukuba, Ibaraki 305-8569. Fax: +81 29 861 8308; Tel: +81 29 861 8336; E-mail: kaori.shigeta@aist.go.jp

b Tokyo Institute of Technology, Department of Energy Sciences, 4259 Nagatsuta, Midori-ku 226-8502 Yokohama, Japan.

† Electronic Supplementary Information (ESI) available: [details of any supplementary information available should be included here]. See DOI: 10.1039/b000000x/

‡ Footnotes should appear here. These might include comments relevant to but not central to the matter under discussion, limited experimental and spectral data, and crystallographic data.

Fig. 1 Schematic of droplet direct injection nebulizer (D-DIN).

Fig. 2 ICP-torch for droplet direct injection nebulizer (D-DIN) system.

Fig. 3 Droplet velocity as a function of back pressure at (a) various valve open times: 0.5, 1.0 and 10 msec, and (b) various nozzle diameters: 30, 50 and 100 μm .

Fig. 4 Emission profiles of Ar atomic line (Ar I 425.11 nm), H_β line (486.13 nm) and Ar excitation temperature with injection of droplets generated from ultra-

1 pure water. Emission intensities were observed by side-on observation (RF
2 power, 1000 W; Droplet volume, 5.5 nL (220 μm); droplet introduction frequency,
3 10 Hz).

4 Fig. 5 Emission profiles of H_{β} line (486.13 nm) as a function of (a) RF power, (b)
5 valve open time, and (c) back pressure with injection of droplets generated from
6 ultra-pure water. RF power is 1000W. The droplets were injected basically under
7 the following condition: nozzle tip diameter, 100 μm ; back pressure, 0.05 MPa;
8 valve open time, 0.5 ms. Emission intensities were observed by side-on
9 observation.

10 Fig. 6 Variation in emission profiles of Na atomic line (Na I 588.99 nm) and H_{β}
11 line (486.13 nm) with carrier gas flow of (a) 0 L min^{-1} , (b) 0.4 L min^{-1} , (c) 0.6 L min^{-1}
12 and (d) 0.8 L min^{-1} , with injection of droplets generated from 10 $\mu\text{g mL}^{-1}$ Na
13 standard solution Emission intensities were observed by end-on observation. (RF
14 power, 700 W; Droplet volume, 4.7 nL (210 μm)).

15 Fig. 7 Emission profile of (a) Na I 588.99 nm, (b) Mg II 280.27 nm, and (c) Sr II
16 407.77 nm, with injection of a series of droplets generated from 10 $\mu\text{g mL}^{-1}$ Na,
17 Mg and Sr standard solution. Emission intensities were observed by side-on
18 observation (RF power, 700 W; carrier gas flow, 0.4 L min^{-1} ; Droplet volume, 15
19 nL (300 μm); droplet introduction frequency, 0.5 Hz).

20 Fig. 8 Emission intensities of Na I 588.99 nm from a single droplet containing
21 3300 yeast cells. Emission intensities were observed by side-on observation (RF
22 power, 700 W; carrier gas flow, 0.4 L min^{-1} ; Droplet volume, 15 nL (300 μm)).

ESI

23 Fig. I The experimental arrangement used for atomic emission spectrometry by
24 (a) side-on observation, and (b) end-on observation.

25 Fig. II Emission profile of (a) Na I 588.99 nm, (b) Mg II 280.27 nm, and (c) Sr II
26 407.77 nm, with injection of a single droplet generated from 10 $\mu\text{g mL}^{-1}$ Na, Mg
27 and Sr standard solution. Droplet volume is 15 nL (300 μm); droplet introduction
28 frequency is 0.5 Hz. Emission intensities were observed by side-on observation
29 (RF power, 700 W; carrier gas flow, 0.4 L min^{-1} ; Droplet volume, 15 nL (300 μm)).

-
- 30
31 1 L. A. Finney and T. V. O'Halloran, *Science*, 2003, **300**, 931.
32 2 H. Haraguchi, *J. Anal. At. Spectrom.*, 2004, **19**, 5.
33 3 K. H. Thompson and C. Orvig, *Science*, 2003, **300**, 936.
34 4 H. Haraguchi, A. Ishii, T. Hasegawa, H. Matsuura and T. Umemura,
35 *Pure Appl. Chem.*, 2008, **80**, 2595.
36 5 D. R. Bandura, V. I. Baranov, O. I. Ornatsky, A. Antonov, R. Kinach,
37 X. Lou, S. Pavlov, S. Vorobiev, J. E. Dick and S. D. Tanner, *Anal.*
38 *Chem.*, 2009, **81**, 6813.
39 6 S. C. Bendall, E. F. Simonds, P. Qui, E. D. Amir, P. O. Krutzik, R.
40 Finck, R. V. Bruggner, R. Melamed, A. Trejo, O. Ornatsky, R. S.
41 Balderas, S. K. Plevritis, K. Sachs, D. Pe'er, S. D. Tanner and G. P.
42 Nolan, *Science*, 2011, **332**, 687.
43 7 F. Li, D. W. Armstrong and R. S. Houk, *Anal. Chem.*, 2005, **77**,
44 1407.
45 8 K. S. Ho and W. T. Chan, *J. Anal. At. Spectrom.*, 2010, **25**, 1114.
46 9 A. S. Groombridge, S. Miyashita, S. Fujii, K. Nagasawa, T. Kahashi,
47 M. Ohata, T. Umemura, A. Takatsu, K. Inagaki, and K. Chiba, *Anal.*
48 *Sci.*, 2013, **29**, 597.
49 10 F. Laborda, J. Jiménez-Lamana, E. Bolea and J. R. Castillo, *J. Anal.*
50 *At. Spectrom.*, 2013, **28**, 1220.
51 11 G. M. Hieftje and H. V. Malmstadt, *Anal. Chem.*, 1968, **40**, 1860.
52 12 J. B. French, B. Etkin and R. Jong, *Anal. Chem.*, 1994, **66**, 685.
53 13 J. W. Olesik and S. E. Hobbs, *Anal. Chem.*, 1994, **66**, 3371.
54 14 S. Groh, C. C. Garcia, A. Murtazin, V. Horvatic and K. Niemax,
55 *Spectrochim. Acta, Part B*, 2009, **64**, 247.
56 15 J. O. O. v. Niessen, J. N. Schaper, J. H. Petersen and N. Bings, *J.*
57 *Anal. At. Spectrom.*, 2011, **26**, 1781.
58
59
60 16 K. Shigeta, H. Traub, U. Panne, A. Okino, L. Rottmann and N.
Jakubowski, *J. Anal. At. Spectrom.*, 2013, **28**, 646.
17 K. Shigeta, G. Koellensperger, E. Rampler, H. Traub, L. Rottmann, U.
Panne, A. Okino and N. Jakubowski, *J. Anal. At. Spectrom.*, 2013, **28**,
637.
18 S. Gschwind, L. Flamigni, J. Koch, O. Borovinskaya, S. Groh, K.
Niemax and D. Gunther, *J. Anal. At. Spectrom.*, 2011, **26**, 1166.
19 B. Franze, I. Streng and C. Engelhard, *J. Anal. At. Spectrom.*, 2012,
27, 1074.
20 Okino, H. Miyahara and G. Ohba, EP 1895286 A1, 2008. US
2009/0297406, 2009.
21 H. Miyahara, K. Shigeta, N. Nakashima, Y. Nagata and A. Okino,
Japan analyst, 2010, **59**, 363.
22 H. Yabuta, H. Miyahara, M. Watanabe, E. Hotta and A. Okino, *J.*
Anal. At. Spectrom., 2002, **17**, 1090.
23 Okino, H. Miyahara, H. Yabuta, M. Watanabe and E. Hotta, in
Colloquium Spectroscopicum Internationale XXXIII 2003, pp. 696-
697.
24 H. Miyahara, T. Doi, Y. Mizusawa, Y. Hayashi, E. Hotta and A.
Okino, in 2004 Winter Conference Plasma Spectrochemistry, 2004,
p. 284.
25 H. Miyahara, T. Doi, Y. Mizusawa, E. Hotta and A. Okino, *Japan*
analyst, 2004, **53**, 817.
26 Montaser, I. Ishii, R. H. Clifford, S. A. Sinex and S. G. Capar, *Anal.*
Chem., 1989, **61**, 2589.
27 R. C. Weast, CRC handbook of chemistry and physics, CRC Press,
Inc, Florida, 1989.
28 L. Ebdon and P. Goodall, *J. Anal. At. Spectrom.*, 1992, **7**, 1111.
29 Y. Kaburaki, A. Namura, Y. Ishihara, T. Iwai, H. Miyahara and A.
Okino, *Anal. Sci.*, **29**, 1147.
30 H. Haraguchi, Basis and application of ICP optical emission
spectrometry, Koudansha, Tokyo, 1986.

Entry gallery

We evaluated the analytical performances of new sample introduction system using a magnetic valve type dispenser, which can generate a large variety of droplet size for stable injection of cell suspension.

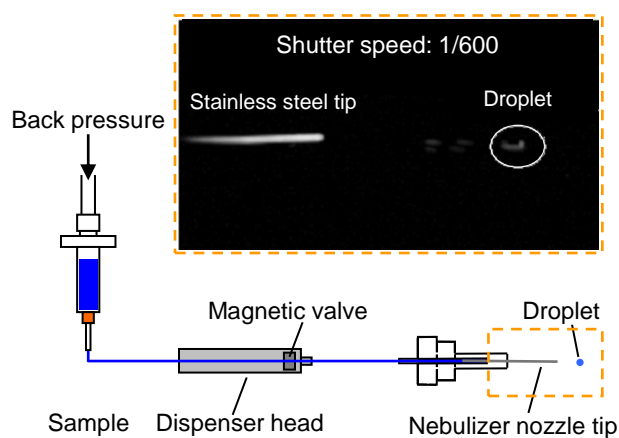
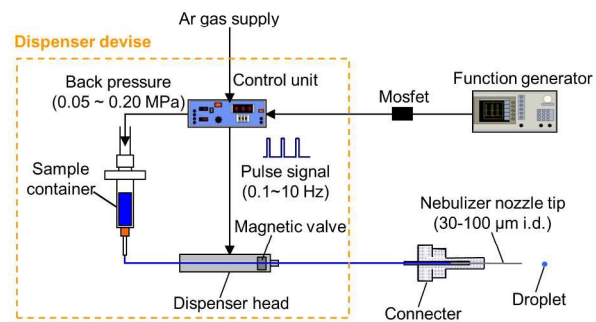


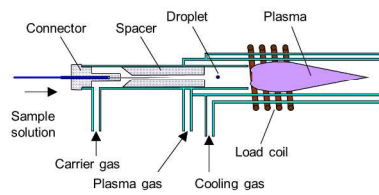
Fig. 1



190x254mm (300 x 300 DPI)

1
2
3
4
5
6
7
8
9
10
11
12
13
14
15
16
17
18
19
20
21
22
23
24
25
26
27
28
29
30
31
32
33
34
35
36
37
38
39
40
41
42
43
44
45
46
47
48
49
50
51
52
53
54
55
56
57
58
59
60

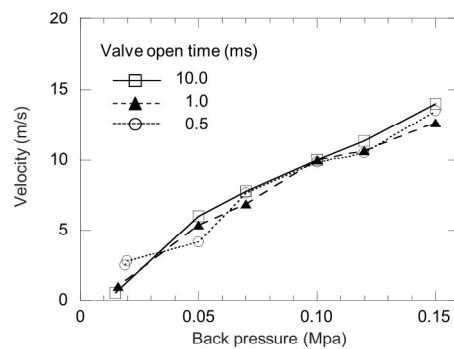
Fig. 2



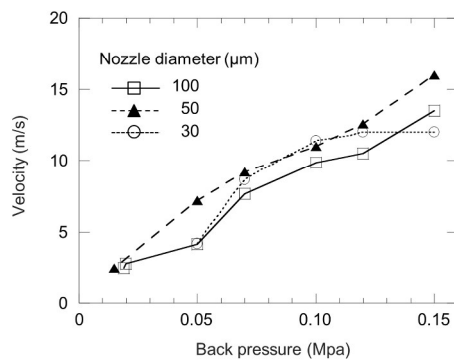
190x254mm (300 x 300 DPI)

Fig. 3

(a) Various valve open time

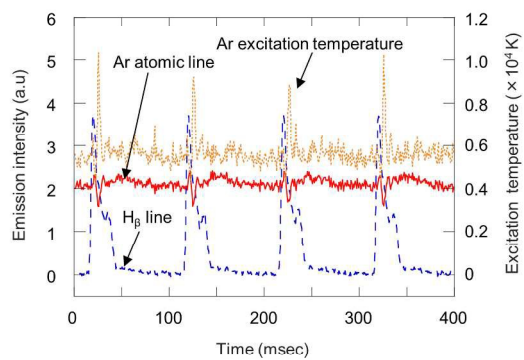


(b) Various nozzle diameter



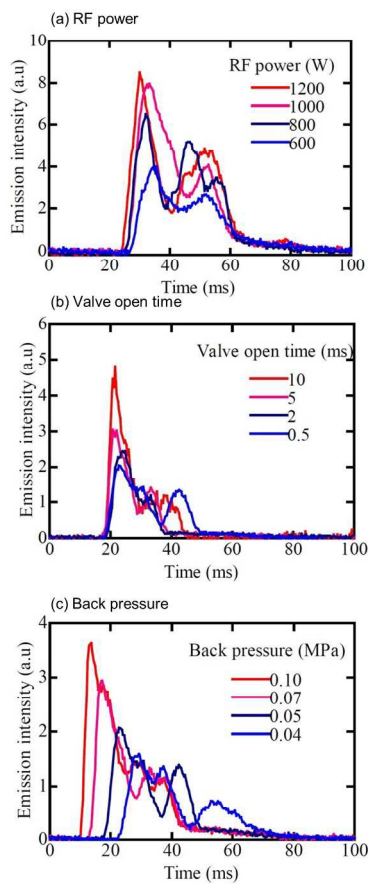
190x254mm (300 x 300 DPI)

Fig. 4



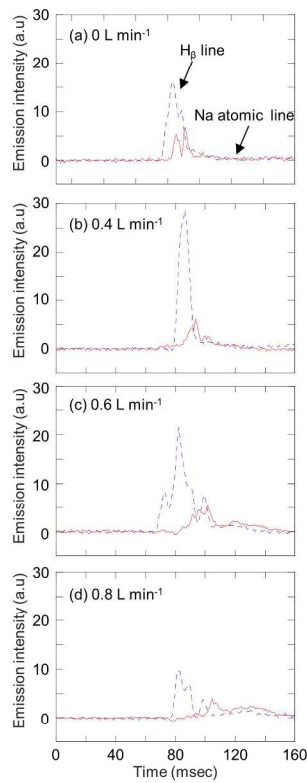
190x254mm (300 x 300 DPI)

Fig. 5



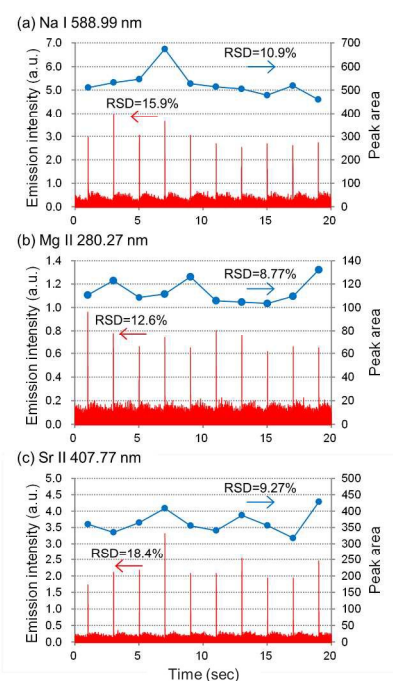
190x254mm (300 x 300 DPI)

Fig. 6



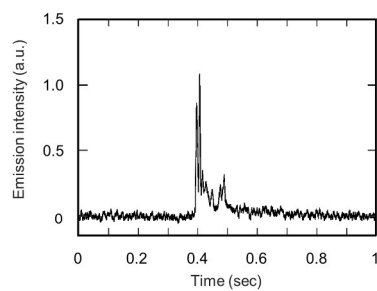
190x254mm (300 x 300 DPI)

Fig. 7



190x254mm (300 x 300 DPI)

Fig. 8



190x254mm (300 x 300 DPI)

1
2
3
4
5
6
7
8
9
10
11
12
13
14
15
16
17
18
19
20
21
22
23
24
25
26
27
28
29
30
31
32
33
34
35
36
37
38
39
40
41
42
43
44
45
46
47
48
49
50
51
52
53
54
55
56
57
58
59
60

Table 1

Table 1 Comparison of relative and absolute limit of detection (LOD) between D-DIN-ICP-AES and conventional ICP-AES. The relative LOD calculated by 3 times the S/N (n=10). Absolute LOD were calculated by multiplying the detection limit (mg L^{-1}) by the droplet volume (μL). ($10 \mu\text{g mL}^{-1}$ Na, Mg and Sr standard solution; Droplet volume, 15 nL (300 μm); Emission intensities were observed by side-on observation)

Isotope	D-DIN ICP-AES			Conventional ICP-AES		
	LOD (ppm)	Absolute LOD (pg)	Sample volume (nL)	LOD ²⁹ (ppb)	Absolute LOD (pg)	Sample volume ^a (mL)
			15			0.27
Na	1.35	20.3		2	333	
Mg	3.77	56.5		0.1	50	
Sr	1.37	20.6		0.1	30	

^a Total amount of sample consumption during measurement time (20 s).

190x254mm (300 x 300 DPI)